PCCC-8

An Integrated Modelling Framework for Pilot-Scale Electrochemical Regeneration of Alkaline CO_2 Capture Solvents

Fariborz Shaahmadi, Katia Piscina, Sotirios Efstathios Antonoudis, Qingdian Shu, Sara Vallejo Castaño, Grigorios Itskos, Konstantinos Atsonios, Susana Garcia, Sai Hema Vinjarapu, Philip Loldrup Fosbøl, Mijndert van der Spek

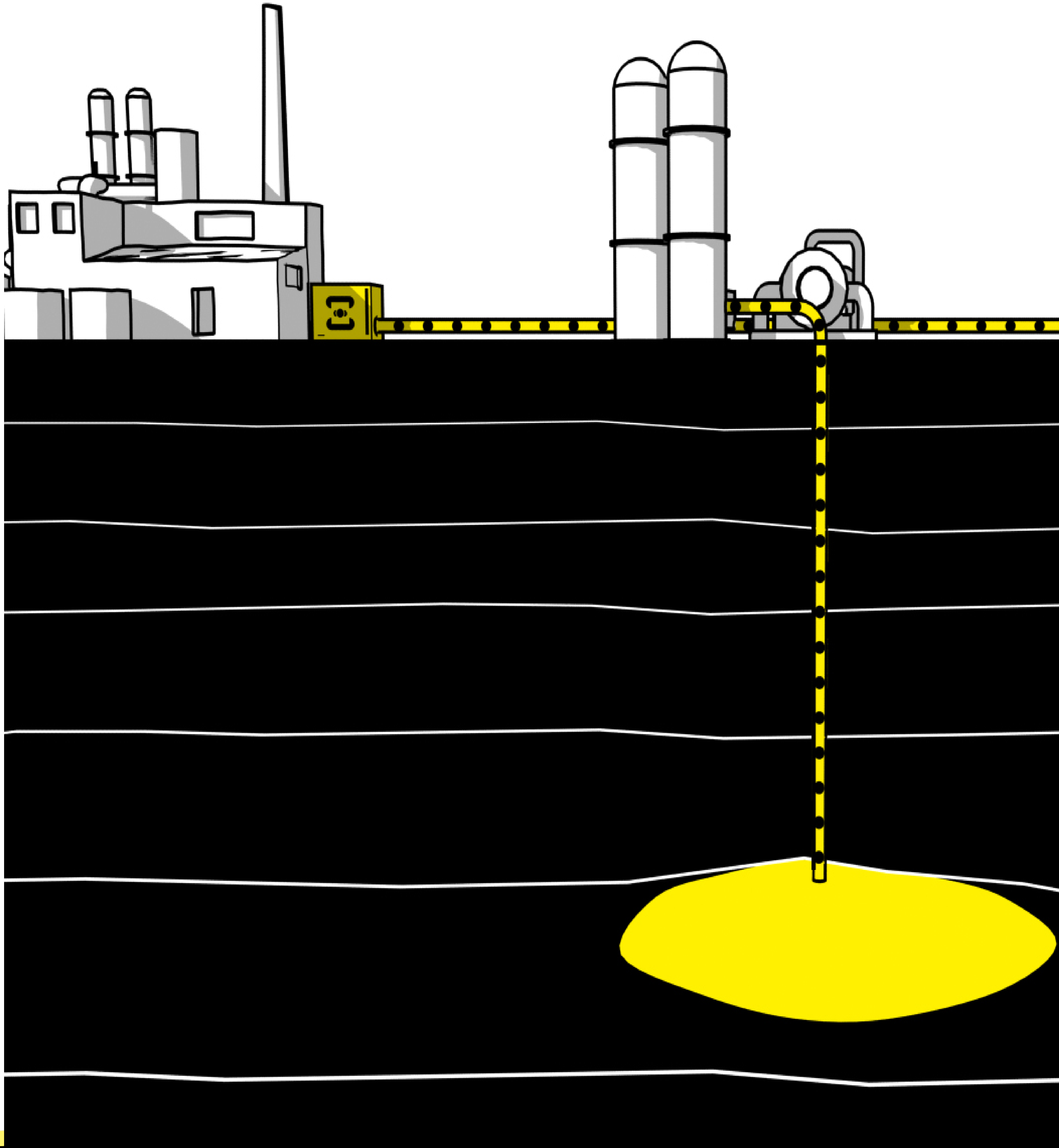

ConsenCUS

This project has received funding from the European Union's Horizon 2020 research and innovation programme under grant agreement No 101022484

Introduction

Global Warming Trends:

- Significant rise in global average surface temperature.
- Increased frequency of extreme weather events.

Consequences of Climate Change:

- Severe impacts on agriculture, biodiversity, and human health.
- Economic losses and social disruption.

Need for Action:

- Importance of reducing carbon emissions.
- Urgent need for sustainable solutions to mitigate climate change effects.
- Development of innovative technologies for CO_2 capture and utilization.

CO_2 Capture

- Potential of absorption in alkaline solutions coupled with electrochemical regeneration as a solution.
- A sorbent with high absorption capacity and less volatility and toxicity.
- KOH reacts with CO_2 to form potassium carbonate/bicarbonate solution (K_2CO_3/$KHCO_3$).
- An electrochemically-driven pH swing to desorb CO_2 and regenerate the solvent.
- There is no an available model to simulate the process.

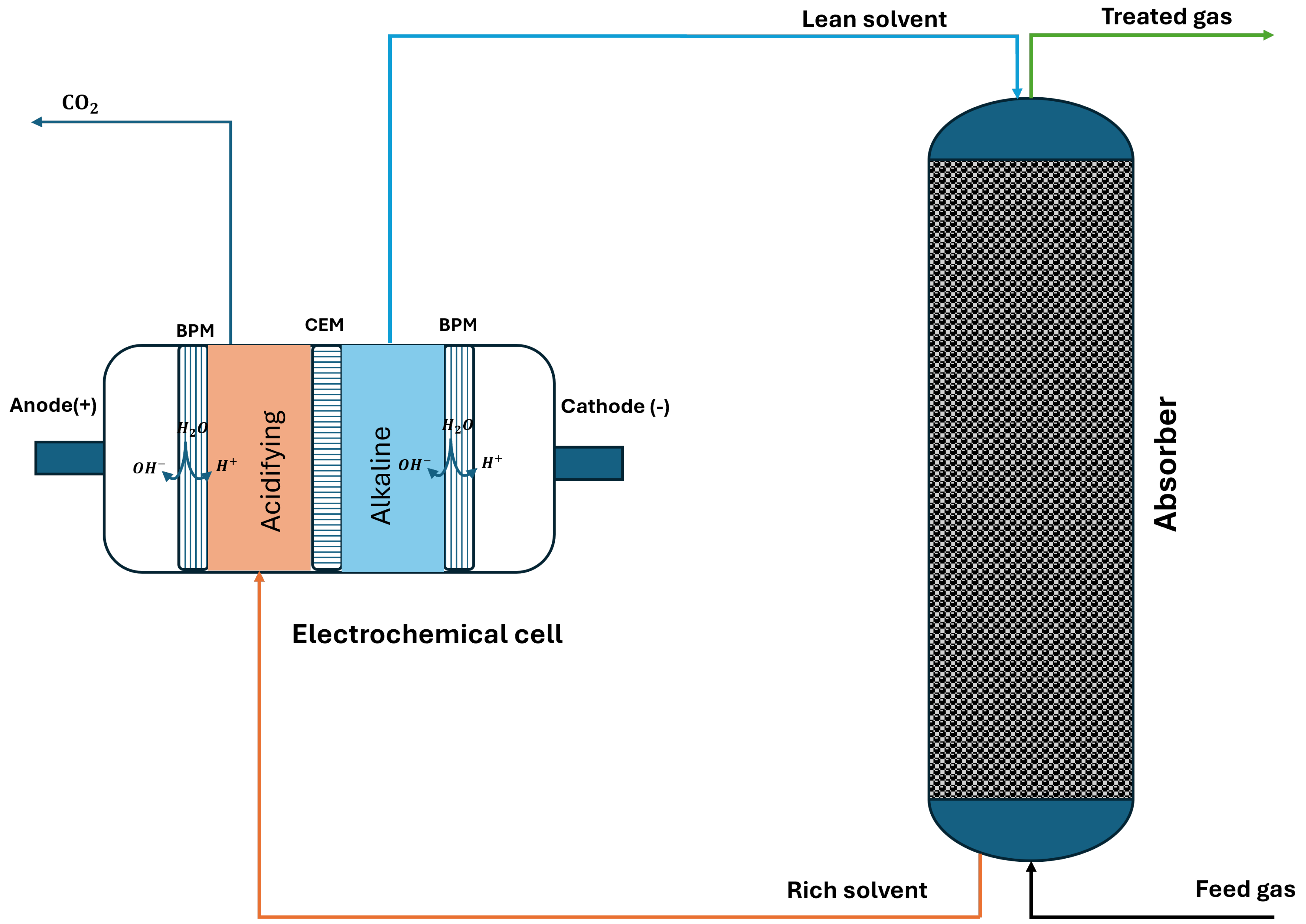

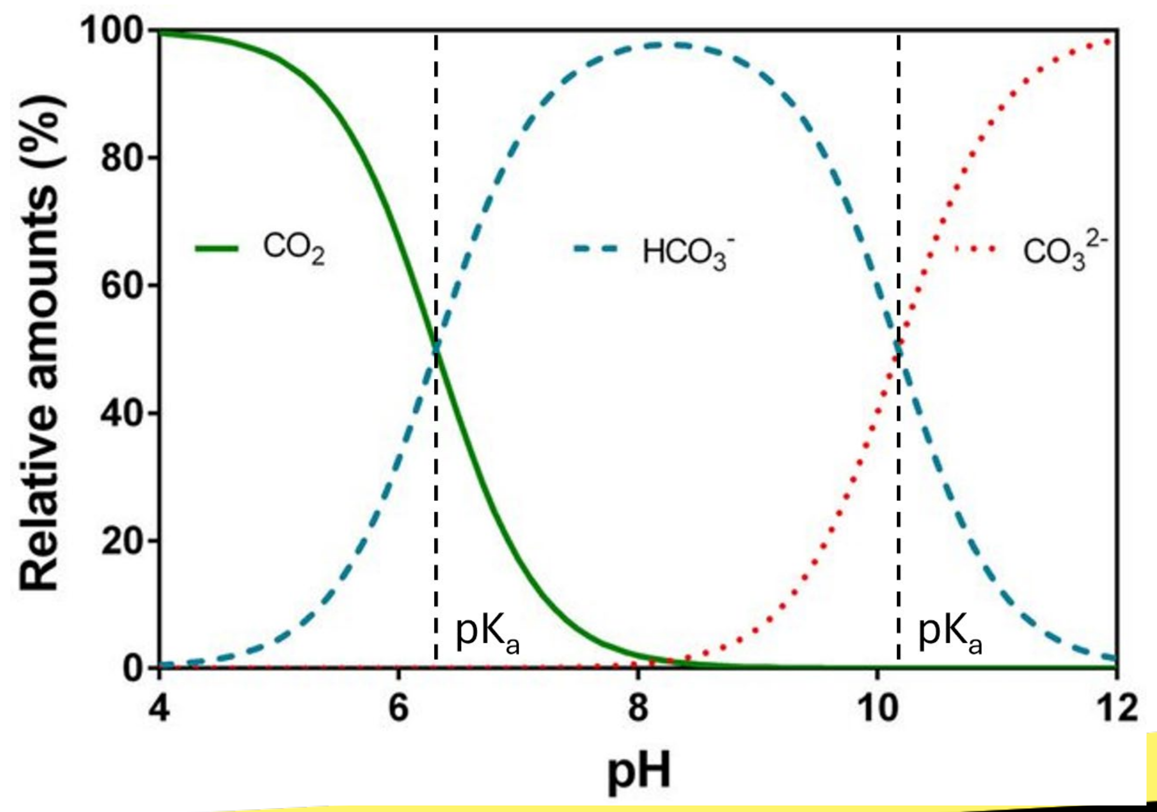

ConsenCUS

Focus Areas

Absorber Modelling:

- Simulation of the absorber unit.
- Key aspects: gas flow rates, solvent flow rates, and capture efficiency.
- Importance: Optimizing these parameters to achieve high CO_2 capture efficiency.

- **Electrochemical Cell (E-Cell) Modelling:**
- Role of E-Cell in the CO_2 desorption process during solvent regeneration.
- Factors: Current density, resistive heating, and bubble formation.

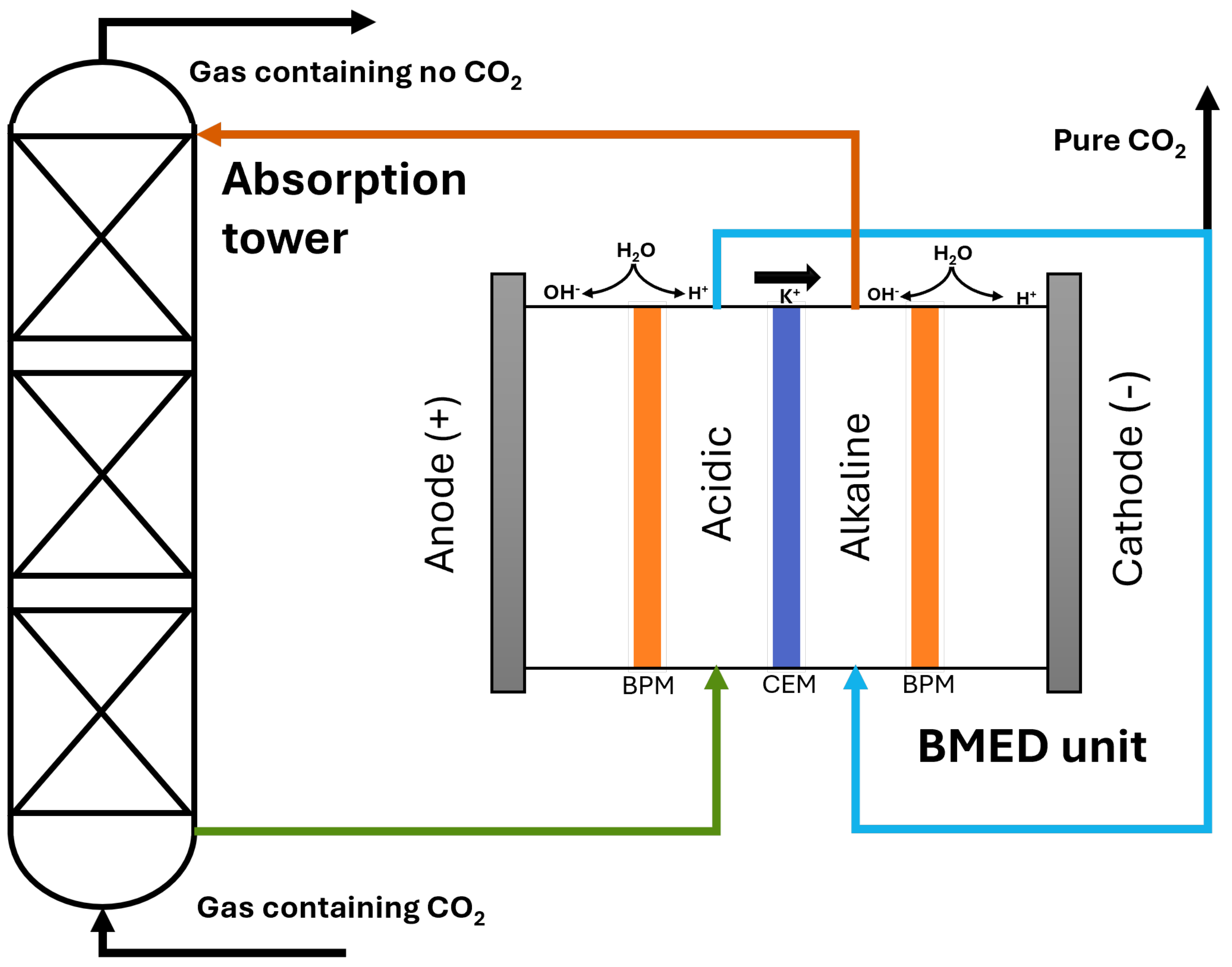

ConsenCUS

Integration of electrochemical regeneration into ASPEN Plus enables comprehensive modelling of CO_2 capture processes.

Absorber Simulation

- Aspen Plus is used for the simulation
- Chemical species present in the process
- Vapour-Liquid Equilibria (VLE)

$$y_i \varphi_i^v P = x_i \gamma_i^* H_i$$

- Experimental data from literature containing $K_2CO_3/CO_2/H_2O$
- Thermodynamic model: Electrolyte NRTL
- The ionic reactions
- Modifications made to equilibrium reactions and kinetics based on previous work.

ID	Name
CO2	CARBON-DIOXIDE
N2	NITROGEN
WATER	WATER
KOH	POTASSIUM-HYDROXIDE
K2CO3	POTASSIUM-CARBONATE
KHCO3	POTASSIUM-BICARBONATE
H3O+	H3O+
K+	K+
OH-	OH-
HCO3-	HCO3-
CO3--	CO3--

	Reactions
1	$2H_2O_{(l)} \leftrightarrow H_3O^+_{(aq)} + OH^-_{(aq)}$
2	$CO_{2(aq)} + OH^-_{(aq)} \rightarrow HCO^-_{3(aq)}$
3	$HCO^-_{3(aq)} \rightarrow CO_{2(aq)} + OH^-_{(aq)}$
4	$CO_{2(aq)} + 2H_2O_{(l)} \rightarrow H_3O^+_{(aq)} + HCO^-_{3(aq)}$
5	$H_3O^+_{(aq)} + HCO^-_{3(aq)} \rightarrow CO_{2(aq)} + 2H_2O_{(l)}$
6	$HCO^-_{3(aq)} + H_2O_{(l)} \leftrightarrow CO^{2-}_{3(aq)} + H_3O^+_{(aq)}$
7	$KOH \leftrightarrow K^+ + OH^-$
8	$K_2CO_3 \leftrightarrow 2K^+ + CO_3{}^{2-}$
9	$KHCO_3 \leftrightarrow K^+ + HCO_3{}^-$

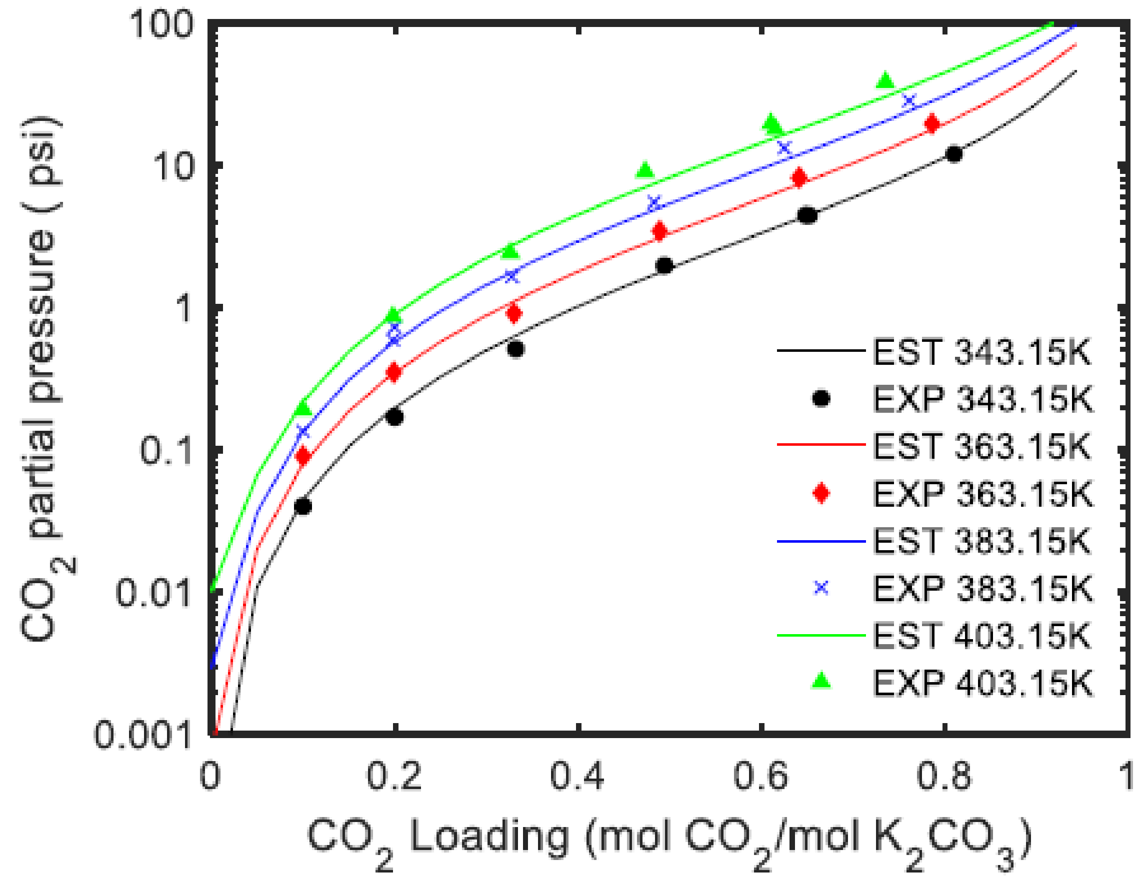

Figure- CO_2 partial pressure of K_2CO3-CO_2-H_2O (equivalent concentration of K_2CO_3=30%), experimental data from Tosh et al. [1].

ConsenCUS

Electrochemical Cell (Electrolyser) Simulation

ASPEN Custom Modeller (ACM) is applied.

Main assumptions made in this work:

- The proton generation is assumed to occur directly from water and not from hydrogen.
- All species are assumed at equilibrium state.
- Only CO_2 desorption considered due to the negligible solubility of H_2 and other potentially dissolved gases.

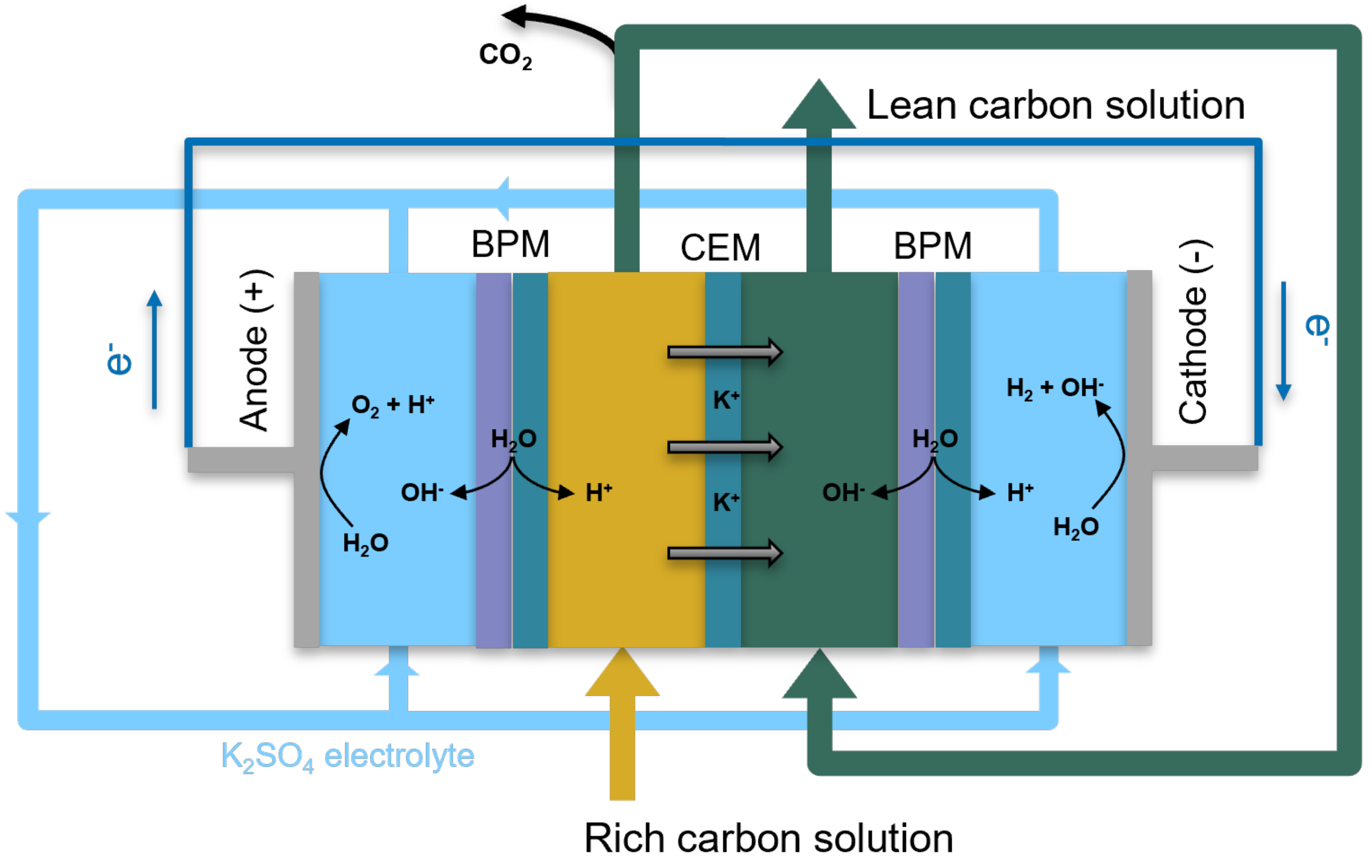

The electrochemical cell model incorporates multiple phenomena

PCCC-8

ConsenCUS

PCCC-8

Electrochemical Cell (Electrolyser) Simulation

- Nernst-Planck equations for the flux (mol s^{-1} m^{-2}) describe the movement of ions across the membrane:

$$J_{K^+} = -D\, c_x \left(\frac{df_{K^+}}{dx} + f_{K^+}\frac{d\Phi}{dx}\right)$$

$$J_{H^+} = -a\, D\, c_x \left(\frac{df_{H^+}}{dx} + f_{H^+}\frac{d\Phi}{dx}\right)$$

- Total current density must satisfy the ionic current density through the CEM:

$$j_c = (J_{K^+} + J_{H^+})\, F$$

- Mass conservation equation over the membrane is

$$J_{K^+} = \frac{Q}{A}\left(C_{K^+}^{in} - C_{K^+}\right)$$

- Inclusion of temperature dependence on Henry's Law, resistive heating across BPMED chamber, and bubble formation in the model.

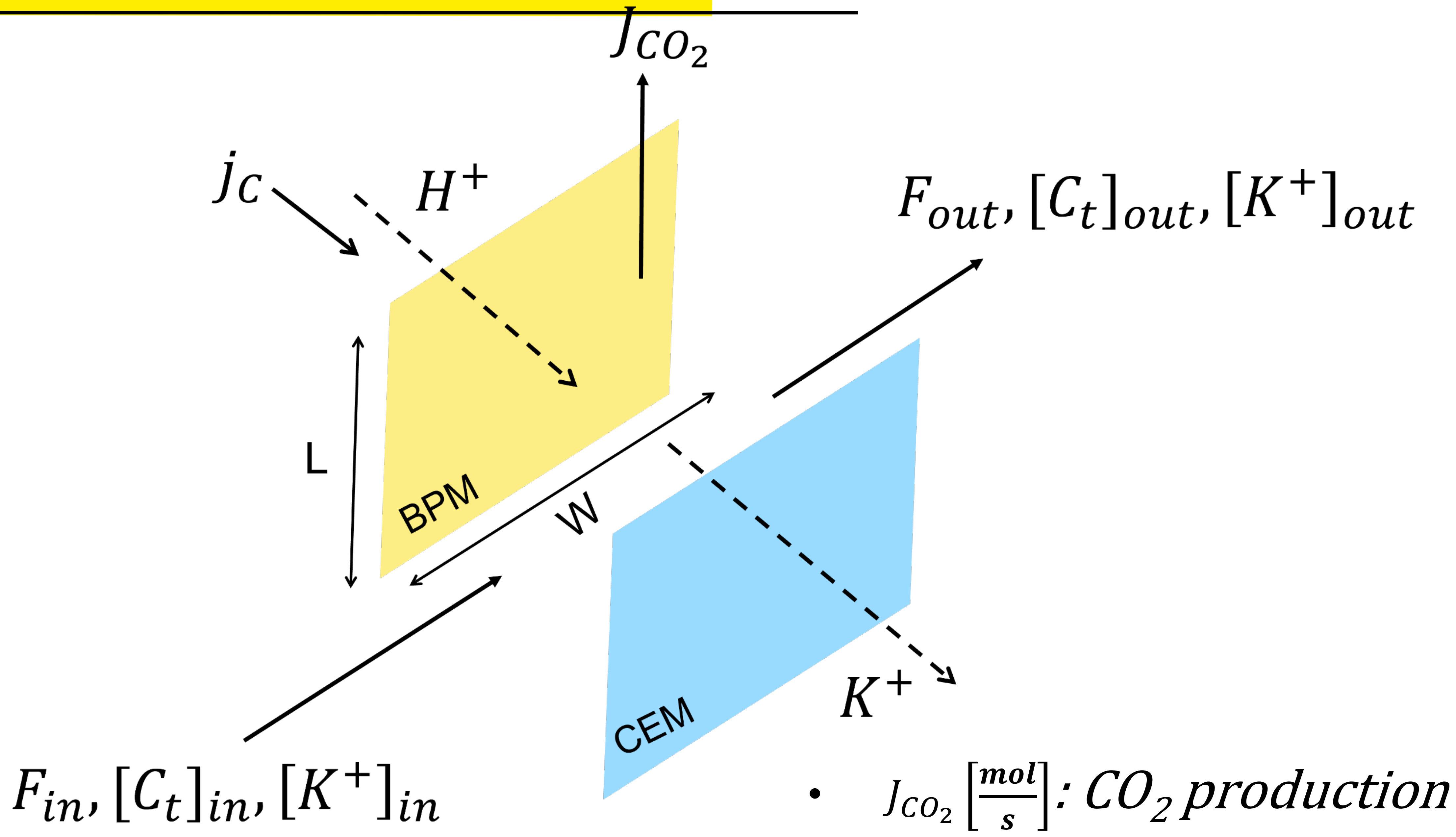

- $J_{CO_2}\left[\frac{mol}{s}\right]$: CO_2 production rate
- $i\left[\frac{C}{s\,m^2}\right]$: Current density
- $A_m[m^2]$: Membrane area
- N: Number of unit cells
- $F\left[\frac{C}{mol\ e^-}\right]$: Faraday constant
- η_i: Current efficiency
- α : carbon loading

ConsenCUS

Integration of electrochemical regeneration into Aspen Plus involves complex thermodynamics and kinetics.

Key performance indicators

- Key Performance Indicators (KPIs) are essential for evaluating the effectiveness and efficiency of CO_2 capture processes.
- Capture efficiency, specific energy consumption, and CO_2 production rate ($\dot{J}_{CO_2}$) are crucial KPIs.

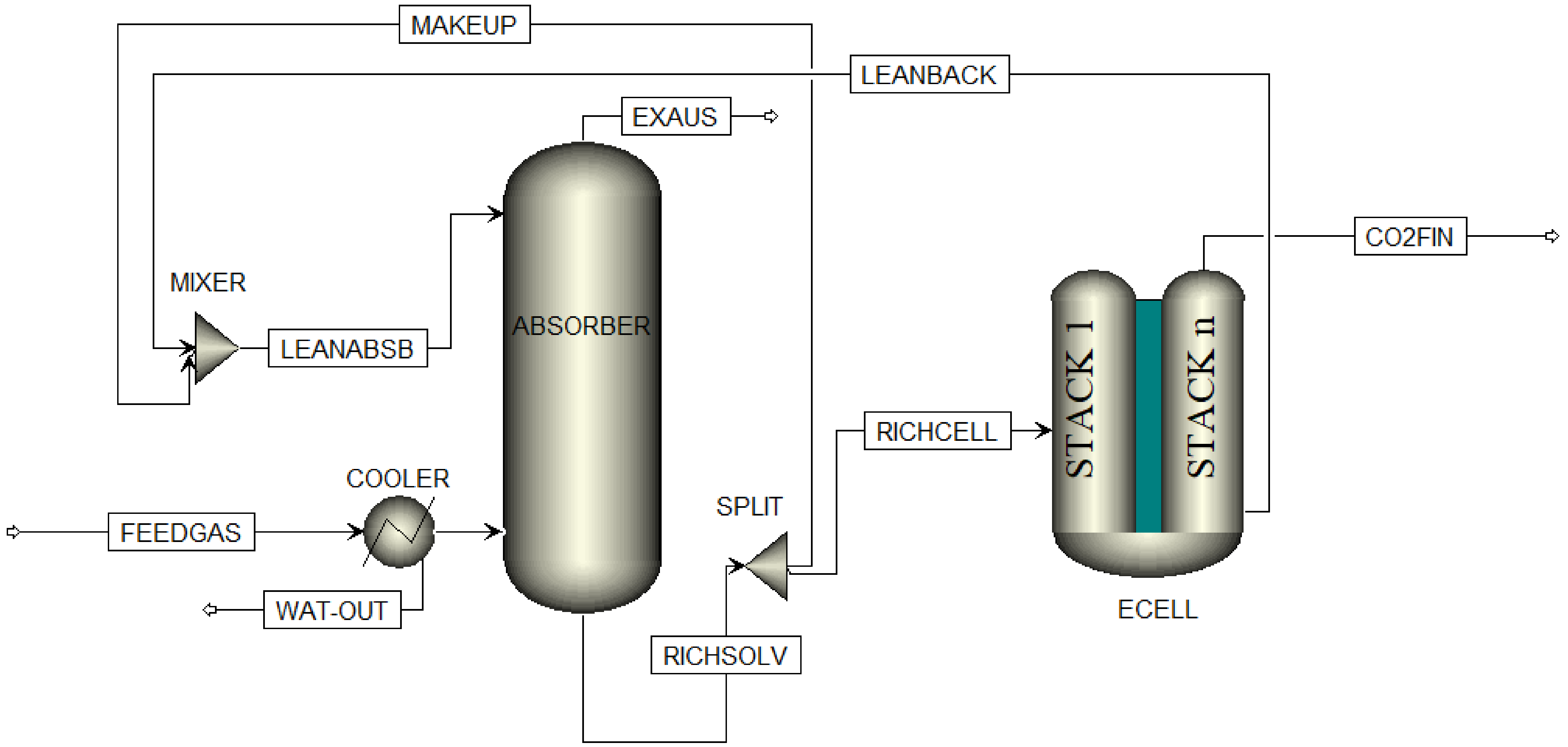

- Capture efficiency

$$\eta_{CO_2\,capture}(\%) = \frac{y_{CO_2,in} - y_{CO_2,out}}{y_{CO_2,in}}$$

- Specific Energy Consumption

$$SEC = \frac{V_{total} j_c A_a}{\dot{J}_{CO_2}}$$

ConsenCUS

These KPI's can be evaluated by experimental results.

Key performance indicators

- Load Ratio:

$$L_{K^+} = \frac{j_C.A}{C_{K^+}.Q.F}$$

- The K+ load ratio (L_{K+}) is a dimensionless parameter that describes the ratio between the potential transport of K^+ at a given current density and the amount of K^+ fed into the system.
- In principle, when L_{K+}= 1, the current in the cell is sufficient to transport all the potassium toward the cathode.

ConsenCUS

Rigorous modelling enables evaluation of CO_2 capture process performance.

Validation of the CO2 capture process

- Validation of the electrochemical regeneration model against experimental measurements.
- Alignment between model predictions and experimental data for CO_2 production.

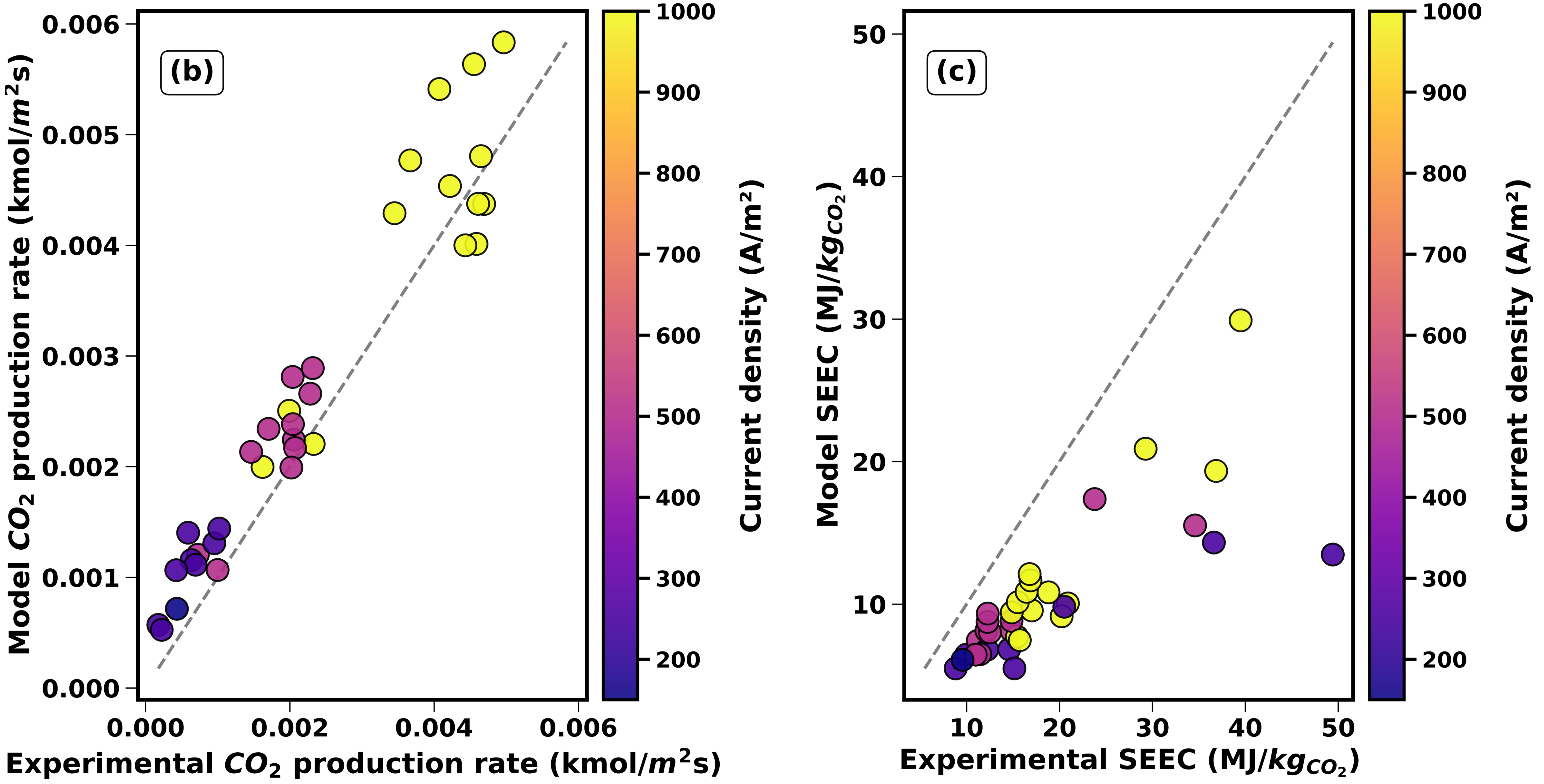

ConsenCUS

Optimal process conditions are essential for the best CO_2 capture KPIs.

Pilot Simulation

- The specifications for the pilot model

component	parameter	value/range
absorber	column type	packed-bed
	packed height	9 m
	diameter	0.6 m
	packing type	Pall ring
	packing diameter	15.875 mm
	packing void fraction	0.9
	packing specific surface area	300 m^2/m^3
	solvent	aqueous KOH
electrochemical cell	configuration	bipolar membrane electrodialysis
	membrane type	BPM-CEM
	membrane (CEM) area	44 cm × 44 cm
	number of stacks	2
	number of cell per stack	126
	fixed charge density (α)	2
	membrane thickness (δ)	4.8×10^{-4} m
	potassium diffusivity	1.96×10^{-9} m^2/s
	proton diffusivity	9.31×10^{-9} m^2/s
	anode (cathode) thickness (d)	0.25×10^{-2} m
	current density	10–150 mA/cm^2

Results and Discussion

3.5% CO_2 in flue gas, 200 kg/h flow rate, varying L/G ratios

- **L/G Ratio & Efficiency**
  Higher L/G (2–5) increases CO_2 capture (up to 100% at L/G = 5) but raises energy use.
- **SEEC vs. Current Density**
  SEEC grows with current density and L/G; higher L/G demands more energy for regeneration.
- **Optimal Load Ratios**
  Minimum energy at load ratios: 0.86 (L/G = 2), 0.83 (L/G = 3), 0.84 (L/G = 5).
- **CO_2 Capture Limits**
  Lower L/G (e.g., 2) limits capture to ~60% due to solvent loading constraints.

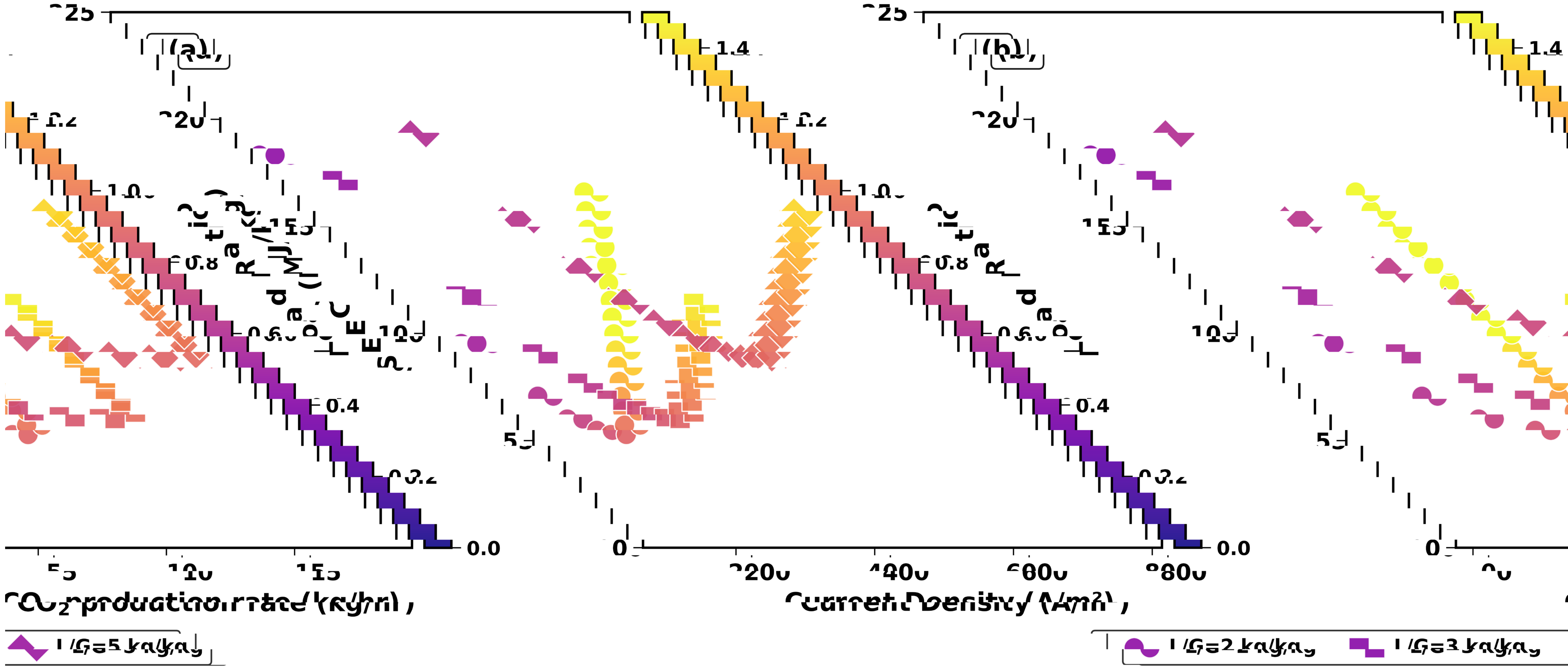

ConsenCUS

Achieving efficient CO_2 desorption requires strategic operational adjustments.

Results and Discussion

CO_2 content in flue gas, varying rich solvent loading and L/G ratios

- **Rich Solvent Loading & SEEC**
  Lower L/G ratios increase rich solvent loading (e.g., 0.58 for CHP, SEEC 3.5 MJ/kg), reducing energy for regeneration; higher L/G dilutes CO_2, raising SEEC.
- **Case Study Performance**
  Cement achieves highest loading (0.78) with minimal SEEC due to strong CO_2 driving force; Magnesite and CHP show higher SEEC at lower loadings (0.5–0.67).
- **Optimal K+ Load Ratios**
  LK+ of 0.8–0.9 balances CO_2 production and ohmic resistance, minimizing energy use; LK+ >1.0 increases resistance, reducing CO_2 output.
- **Ionic Congestion Effects**
  At LK+ >1.0, H+ flux dominates, causing ionic crowding, higher ohmic losses, and wasted heat, increasing energy demands.

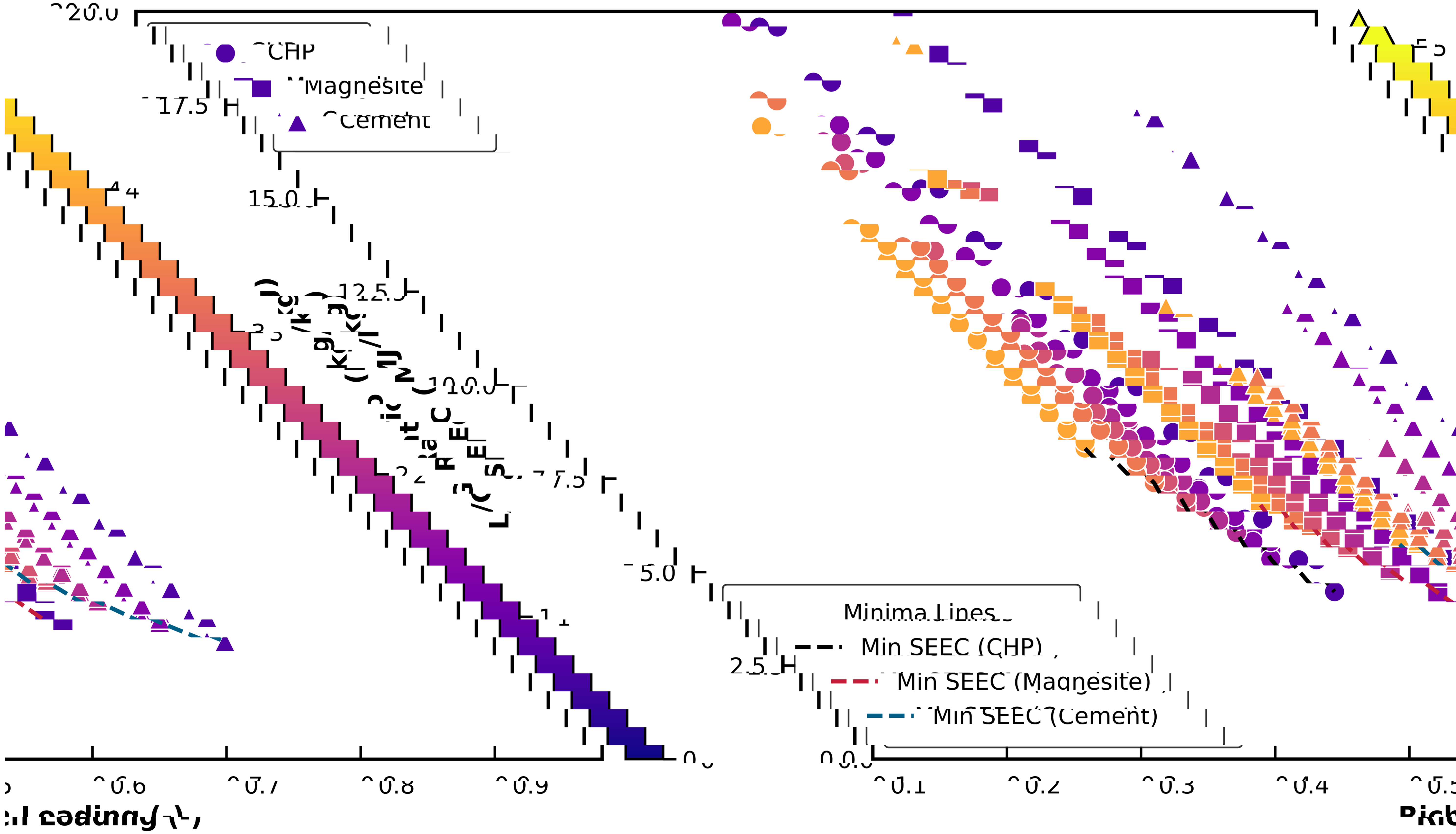

ConsenCUS

Optimal K+ load ratio range for the best performance.

Results and Discussion

Optimal LK+ = 0.8–0.9, varying L/G ratios and current densities

- **CHP Performance (3.5% CO_2)**
  Low CO_2 content leads to lower CO_2 production rates and higher SEEC, especially at higher L/G ratios.
- **Magnesite Performance (9.1% CO_2)**
  Moderate CO_2 content balances capture efficiency and production rates, with better performance at lower L/G ratios.
- **Cement Performance (13.5% CO_2)**
  High CO_2 content yields highest CO_2 production and capture efficiency with lowest SEEC, optimizing energy u
- **CO_2 Content Impact**
  Higher flue gas CO_2 concentrations enhance overall electrochemical cell performance at optimal LK+ (0.8–0.9).

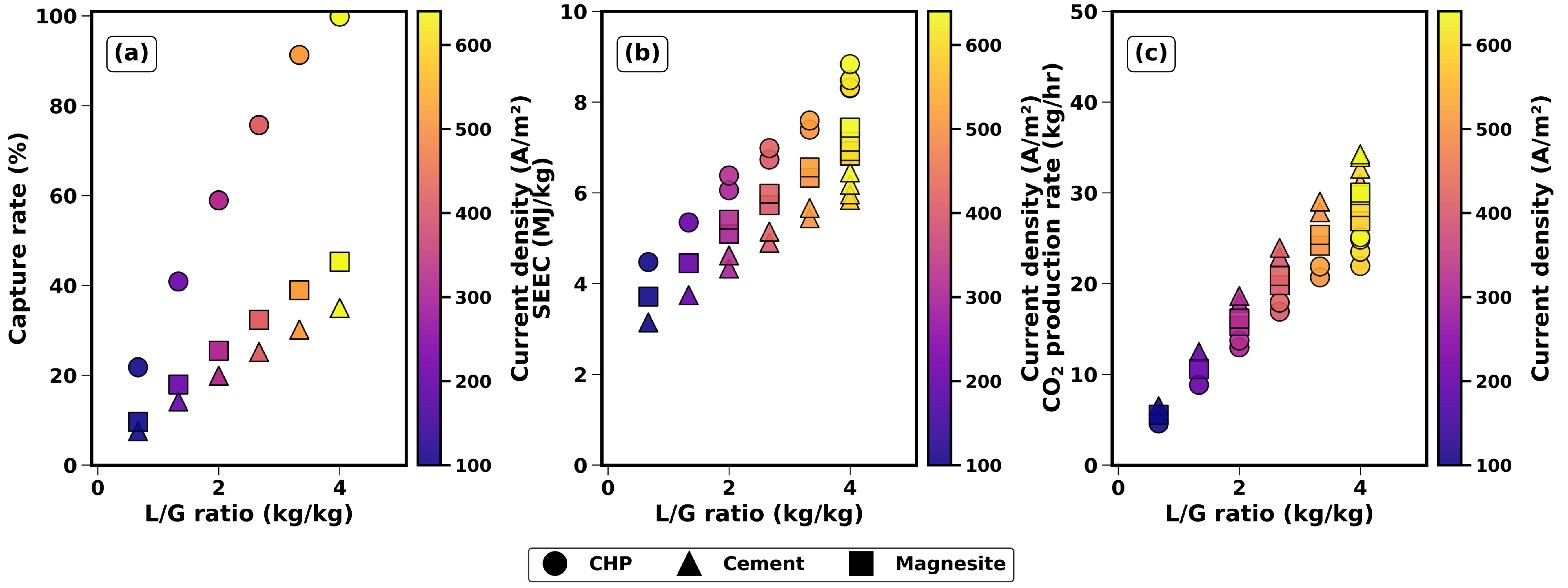

ConsenCUS

Performance at fixed medium current for efficient CO_2 capture and desorption.

Results and Discussion

Fixed current density of 400 A/m², varying L/G and load ratios

- **CHP Capture Efficiency**
  Achieves near 100% capture at high L/G ratios (4.
  but with higher SEEC (7 MJ/kg at L/G ≈ 2.7).
- **Magnesite & Cement Performance**
  Lower capture efficiency (<40% at high L/G, ~20%
  low L/G), with Cement showing better energy efficiency.
- **Optimal L/G Ratio**
  L/G ≈ 2.7 (load ratio 0.8–0.9) minimizes SEEC (<5 MJ/kg for Cement) and maximizes CO_2 production (20 kg/h for Magnesite, 23 kg/h for Cement).
- **Operational Tuning**
  Balancing L/G and load ratios optimizes energy costs and throughput, even with suboptimal capture efficiency.

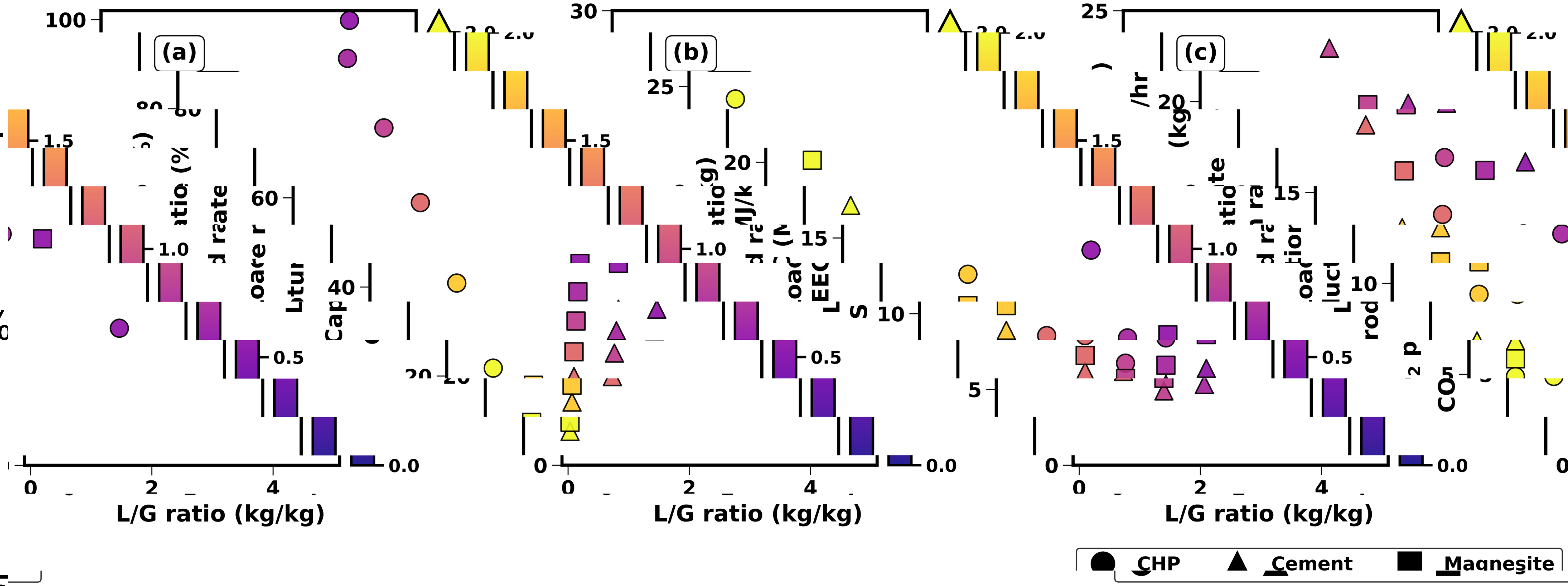

ConsenCUS

Optimal operational conditions are crucial for efficient CO_2 capture and desorption.

PCCC-8

Results and Discussion

Voltage & Power: Model vs. Pilot Data

- **LK+ = 1.0 Performance**
  Pilot data (orange) aligns near 200 V and 40 kW, reflecting efficient ion transport with low membrane resistance.
- **LK+ = 1.4 Deviations**
  Pink data (LK+ = 1.4) shows nonlinear voltage/power increases due to ohmic losses and pH gradient overpotentials.
- **Conductivity Stability**
  Pilot maintains 6–8 S/m conductivity vs. model's 5–35 S/m, attributed to uniform KOH replenishment and limited mixing.

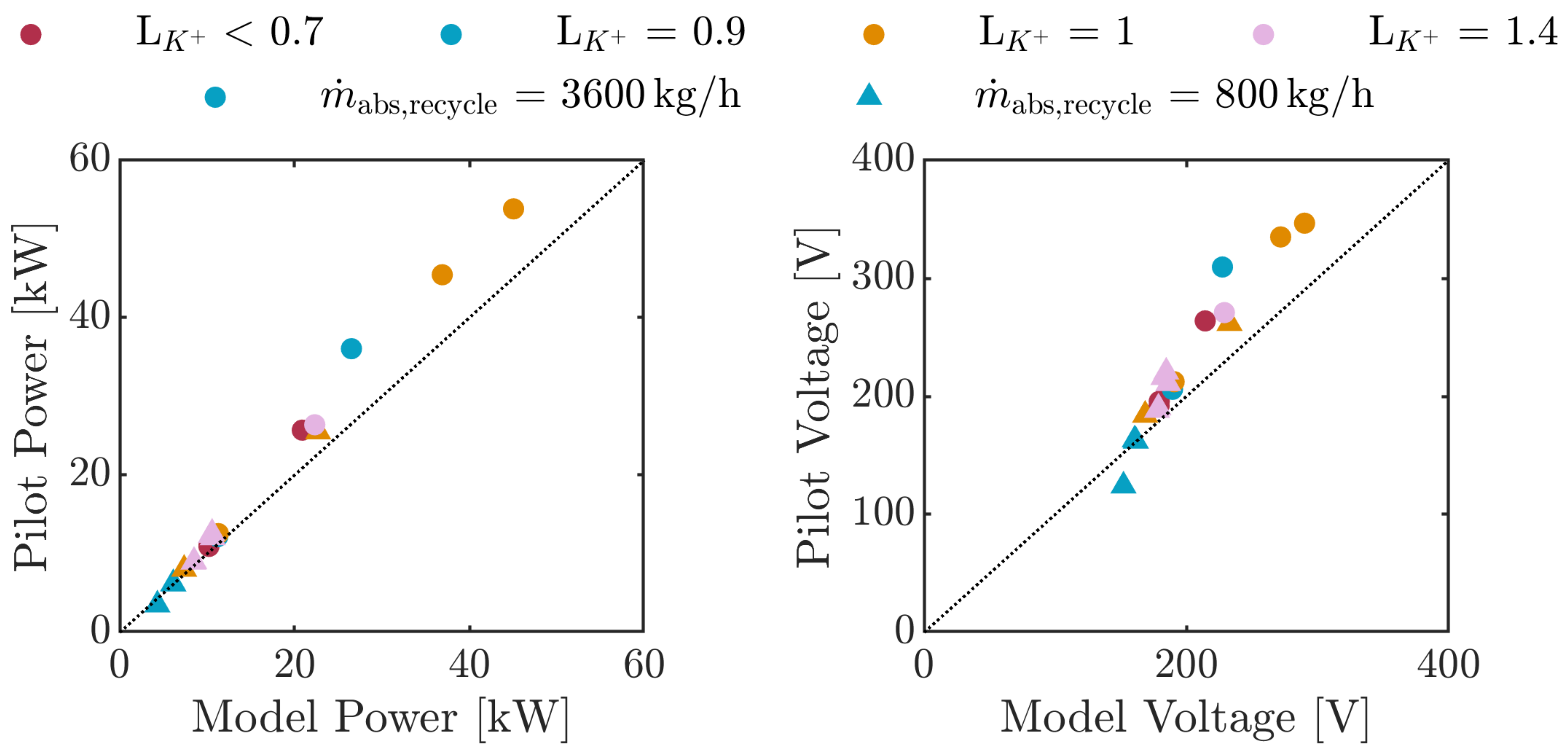

ConsenCUS

Results and Discussion

- **Capture Efficiency**
  Model predicts ~100% efficiency at LK+ – 1.0; pilot data (orange) matches up to 600 A/m² but drops at higher currents due to mixing issues.
- **SEC Discrepancies**
  Model SEC at LK+ = 1.0 is ~7 GJ/tonne CO_2; pilot data (orange) rises to 20 GJ/tonne, reflecting incomplete pH swings.
- **Desorption Limitations**
  Pilot acidic compartment pH (6–7) vs. model pH (3–5) reflects incomplete CO_2 desorption, driven by uneven current and mass transfer issues.

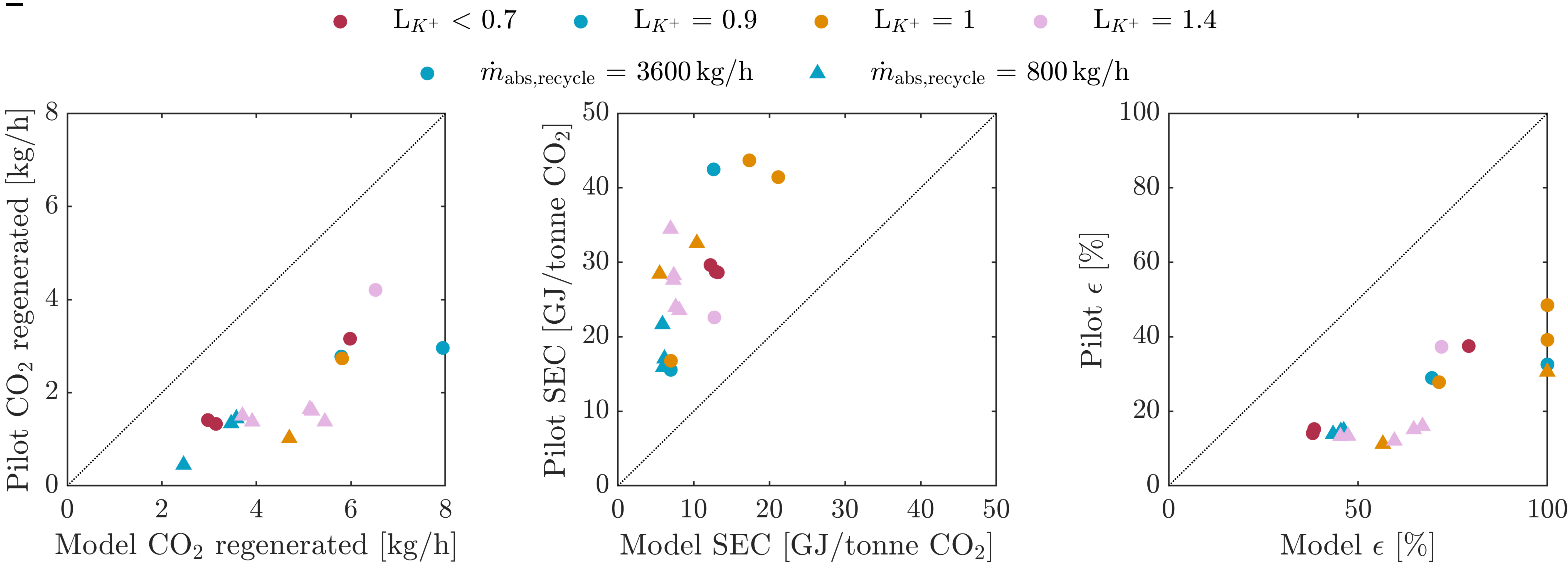

ConsenCUS

Summary

Integrated absorption-electrochemical regeneration model

- **Model Development & Validation**
  Built in Aspen Plus and Custom Modeler, validated with good CO_2 production agreement at low currents (15 mA/cm²), but deviates at higher currents due to unmodeled mass transport and simplified equilibria.
- **L/G Ratio Trade-offs**
  Higher L/G ratios (2–5) increase capture rates (60–100%) but raise SEEC by up to 300%; higher flue gas CO_2 (3.5–13.5%) lowers energy demands.
- **Optimal K+ Loading**
  LK+ = 0.8–0.9 optimizes CO_2 production and minimizes ohmic losses; LK+ > 1.0 increases resistance, reducing efficiency.
- **Industrial Case Studies**
  CHP achieves ~100% capture (60 MJ/kg), while Cement prioritizes throughput (7 kg/h, 10 MJ/kg); tailored parameter optimization is critical.

References

1. J. S. Tosh, J. H. Field, H. E. Benson, and W. P. Haynes, “Equilibrium study of the system potassium carbonate, potassium bicarbonate, carbon dioxide, and water,” 1959.
2. Abdin, Z., C. J. Webb, and E. Maca Gray. 2015. “Modelling and Simulation of a Proton Exchange Membrane (PEM) Electrolyser Cell.” International Journal of Hydrogen Energy 40(39).
3. Ali, Fawaz, and David G. Kwabi. 2022. “ Modeling Electrochemical Direct Air Capture of CO2 Using Redox-Functionalized Electrodes .” ECS Meeting Abstracts MA2022-02(27).
4. Cao, X., Huang, X., Liang, P., Xiao, K., Zhou, Y., Zhang, X. and Logan, B.E., 2009. A new method for water desalination using microbial desalination cells. Environmental science & technology, 43(18), pp.7148-7152.
5. Chae, K.J., Choi, M., Ajayi, F.F., Park, W., Chang, I.S. and Kim, I.S., 2008. Mass transport through a proton exchange membrane (Nafion) in microbial fuel cells. Energy & Fuels, 22(1), pp.169-176.
6. Rastegar and Ghaemi, 2022, “CO2 absorption into potassium hydroxide aqueous solution: experimental and modeling,” Heat Mass Transf. und Stoffuebertragung, 58(3), 365–381.
7. Sabatino, Francesco, Mayank Mehta, Alexa Grimm, Matteo Gazzani, Fausto Gallucci, Gert Jan Kramer, and Martin Van Sint Annaland. 2020. “Evaluation of a Direct Air Capture Process Combining Wet Scrubbing and Bipolar Membrane Electrodialysis.” Industrial and Engineering Chemistry Research 59(15).
8. Seo, H., & Hatton, T. A. 2023. Electrochemical direct air capture of CO2 using neutral red as reversible redox-active material. Nature Communications, 14(1), 313.
9. Shu, Qingdian, Louis Legrand, Philipp Kuntke, Michele Tedesco, and Hubertus V. M. Hamelers. 2020. “Electrochemical Regeneration of Spent Alkaline Absorbent from Direct Air Capture.” Environmental Science and Technology 54(14).
10. Zhang, X., Li, X., Zhao, X. and Li, Y., 2019. Factors affecting the efficiency of a bioelectrochemical system: a review. RSC advances, 9(34), pp.19748-19761.

ConsenCUS

PCCC-8

Thank you!

ConsenCUS!

ConsenCUS